

## SOME COMMENTS CONCERNING THE PREPARATION OF AND FATIGUE TESTING OF THE AIRCRAFT'S CABLE-CONTROL SYSTEM

Józef Brzęczek 

Department of Aerospace Engineering, Faculty of Mechanical Engineering  
and Aeronautics, Rzeszow University of Technology,  
al. Powstańców Warszawy 12, 35-959 Rzeszów.

[j.brzeczek@prz.edu.pl](mailto:j.brzeczek@prz.edu.pl)

### Abstract

The currently accepted rules that are applied to the aircraft cable-control systems' operational use are based on the reactive maintenance idea and the comparative tests, inspections, and diagnostics performed at the mandatory intervals. Fatigue tests of the aviation cables are commonly conducted by bending in the range of  $\pm 90^\circ$  with constant load. Aircraft cable-control systems are subject to a number of random loads and deformations. Additionally, forces and their values are modified by the wear and tear of cable-pulley raceways, elastic deformations, and changes caused by temperature. The actual values of tension of aviation cable-control systems are relatively low, and bending usually does not exceed the maximum of  $\pm 35^\circ$ . Moreover, the forces characteristic of the control cables are nonlinear functions of the control surface deflection. This means that the typical fatigue tests we employ help with only comparative estimations and acceptance tests. It is not possible to estimate the operational durability of the systems and forecast inspections and diagnoses intervals based on the mentioned results. The present article utilizes the operational profiles of selected aircraft categories to determine the stochastic load-related deflection spectra for the preparation of cable fatigue-testing programs. Operation profiles are built considering a group of aircraft belonging to the same category, performing similar missions, for example, training missions, photogrammetric missions, aircraft towing, e.q., and having a similar share in the total resource. The special stands for the selected cable fatigue tests have been proposed. The cable test stand ensures the real stochastic loads for the cable use and other actual conditions of load. The proposed stand enables the simultaneous testing of more than one cable at different deformation parameters, for example, wrap angles. The results of the proposed method and tests can be used to estimate the operational durability of aviation-control systems as well as for inspection and diagnosis intervals as well.

**Keywords:** aviation cable control systems, cables and ropes fatigue tests, inspection intervals assessment, load spectrum, fatigue life.

**Article category:** research article

## Introduction

Cable-control systems of GA<sup>1</sup> aircraft and gliders will remain in use, owing to the use of the electrical or hydraulic systems being irrational due to the inappropriate costs and complex services involved. Currently, symmetrical loads and bending are used in the fatigue tests of airplane cable-control systems, just like in the tests of elevator ropes<sup>2</sup>. The cable and ropes tests are commonly conducted by bending them in the range of  $\pm 90^\circ$  with a constant load. The mentioned tests are adequate for assessing the operational loads of cable transport systems such as cranes, lifts, vertical and horizontal cable transport, and so on (Brzęczek, 2020; Kubryn et al., 2018; Tytko, 2021). For the ropes and pulleys of transport systems, the described methods are used to assess the wear and for damage evaluation (Hankus & Hankus, 2006; Kubryn et al., 2018; Tytko, 1998, 2021). Typical cables test results are given in Figure 1. Kubryn et al. (2018) and Tytko (1998) could only partially point out to the real wear as a function of the operational measure and fatigue life of the aviation-control systems, and these do not correlate with the real deflections and loads.

The forces transferred by the control system should ensuring stability and control are limited by admissible control are results from surfaces deflections  $\Theta_w$  and values of forces  $P_F$  and flying controls as well, Figure 6. (Brzęczek, 2019; Certification Specifications for CS-23, 2003). The flight stability and the aircraft's control are carried out by changing the moments relative to the CG<sup>3</sup> of the aircraft (Figure 2). Values of the hinge moments are not linear functions of control surface deflection, and it is difficult to precisely determine their actual values as well.

The given dependencies indicate the complexity of the issue with random loads and deformations (see Figures 8 and 9). The characteristics of variability are typical and similar for defined airplane categories, operation profiles, and the in-flight mass and CG position. Real loads of the control systems are modified by the required pretensioning (Certification Specifications for CS-23, 2003). The sum of the pretensioning and the real loads cannot reach a negative value for any permissible flight configuration, including loads generated by doubled control systems (Brzęczek, 2019; Certification Specifications for CS-23, 2003). Specifications (Certification Specifications for CS-23, 2003) also require that the designed systems ensure the positive gradients of the flying controls forces  $P_F$  (steering wheel, control stick, pedals) as a function of their range of displacement  $\Theta_w$  (Figure 6).

---

<sup>1</sup> Acronym of General Aviation

<sup>2</sup> In English-language literature, the ropes with a diameter below of 3/8 in. are referred to as cable or cord and above this diameter are referred as rope. The term "cable" is used in the paper.

<sup>3</sup> Acronym of Center of Gravity

Transmission of hinge moments,  $M_{zaw}$ , (Figure 4) causes the difference in tension between the active and passive cables (Figure 6). The random loads of cables caused a complex state of stresses of the wires: stretching, twisting, and contact pressure loads related to the wrap angles of the cable sheaves  $\theta_L$  (Figures 6 and 13). Variations of the deflections,  $\beta_H$  and  $\delta_H$ , (Figures 4 and 6) are the results of the required configurations of moments:  $M$ ,  $L$ , and  $N$  in flights related to the aircraft's CG (Figures 2 and 8). Results of tests (Kubryn et al., 2018; Figure 1) of aviation cables based on the symmetrical variable loads and bending cycles cannot be used for predicting the service life and unequivocal guidelines for the planning, inspection, and intervals of dianosis. Due to the lack of reliable test results, it is recommended to mandatorily inspect defined areas of cable-control systems, especially for the most-loaded element with relatively short inspection intervals, for example, 25 hr of flight. The regulations (Certification Specifications for CS-23, 2003) also require the visual ongoing inspection of critical elements of cable-control systems.

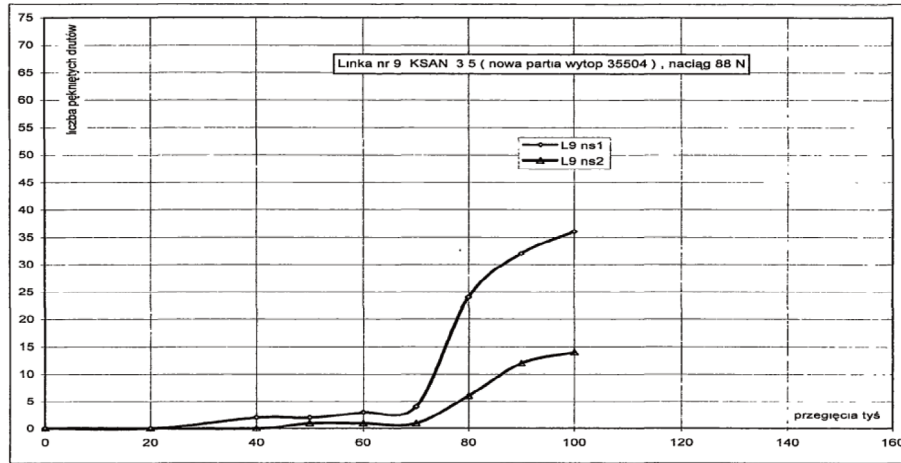


**Figure 1.** The results of the KSAN cable (aviation cable) tests with a diameter of 3.5 mm up to 100,000  $\pm 90^\circ$  bends (Kubryn et al., 2018).

In the present article, only the longitudinal control of the aircraft was analyzed (Figure 2). The resultant value of the force on the tail,  $P_H$ , (Figure 3) ensures longitudinal balance, stability, and flight control. Values of forces in the reference coordinate system of the airplanes are dependent on the flight speed  $v$ , aircraft CG, and their position  $l_h$ , tail angle of attack angle  $\alpha_H$ , deflections  $\beta_H$ , and trimming tab  $\delta_H$  (Figures 3 and 4). The components of the resultant forces on the horizontal tail unit,  $P_H$ , are described using simplified formulas (1–4).

Required values of forces and moments depend on the current aircraft configuration (CG position,  $l_h$ ,  $\alpha_h$ ), control surface deflections ( $\beta_h, \delta_h$ ) and their aerodynamic parameters ( $dC_{zh}$ ,  $dC_{xh}$ ) Figures 2 and 3).

$$C_{ZH} = \frac{dC_{ZH}}{d\alpha_H} (\alpha + \alpha_H + \phi - \varepsilon) + \frac{dC_{ZH}}{d\beta_H} \beta_H + \frac{dC_{ZH}}{d\delta_H} \delta_H \quad (1)$$





Method (a) is closely related to the configuration of the aircraft (see Figure 1), the specific CG, and the profile of its operation. In this study, the second method (b) was analyzed. Data prepared in this way can be further generalized by taking into account the actual values of air speed, mass in flight, and the actual CG position. When converting data into the test loads spectrum, the maximum pre-tension values should be used as a conservative approach (Figure 13).

### Data obtained from the flights

The sources and methods of the loads of the aircraft and the aircraft's control system acquisition are presented in Figures 5 and 7.

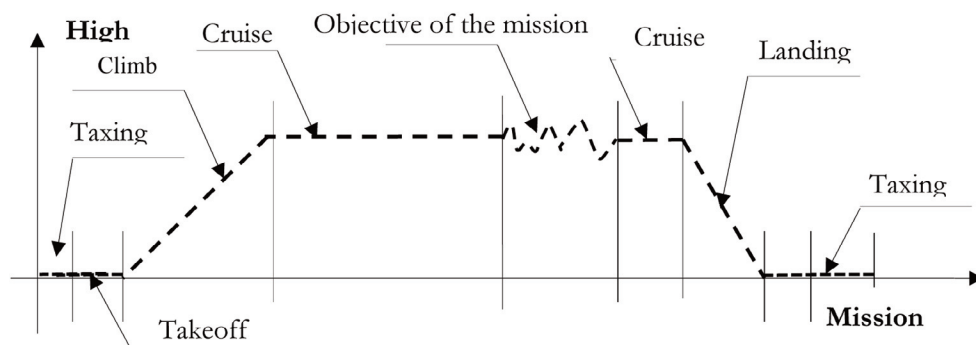


**Figure 5.** Typical flight mission (Brzęczek, 2020).

All real or postulated missions of the selected airplane category allow to define a typical operating profile. The spectrum of the real loads of the aircraft's control systems are divided into:

- controlled loads (depending on the pilot and his training, but determined by the category of the aircraft and their operational profile) are resulting from performed missions;
- controlled loads resulting from the reaction of the pilot or autopilot on flight disturbances (e. g., after gust, engine asymmetry, etc.);
- environmental loads (depending on the state of the atmosphere, the load of the power unit, and the condition of the runway); and
- properties of the aircraft (mass and location of the CG, aerodynamic and power unit characteristics, and stiffness and deformations of the loaded airframe structure) (Brzęczek, 2019).

Actual load values of control system elements (Figure 6) during the flight mission (Figures 7 and 8) should be collected as the result of the operating load spectrum based on the operation aircraft's profile.

The loads of cables are combined with deformations on the pulleys or sliders, and real forces cause a complex state of stress in the strands and wires of the cables (Brzęczek, 2019).

The requirement is for a positive cable tension for each extreme load (Certification Specifications for CS-23, 2003); hence, the need to introduce the  $P_W$  cable pre-tension (Brzeczek, 2019; Certification Specifications for CS-23, 2003) (Eq. (5)).

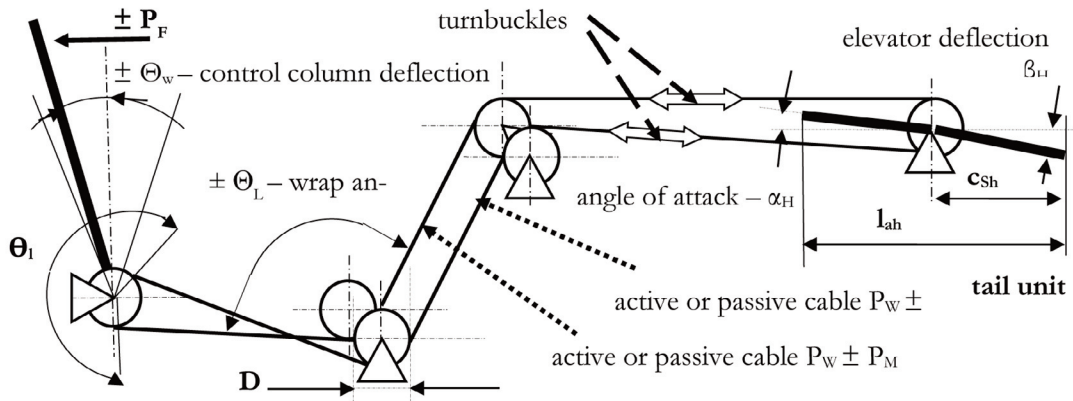


**Figure 6.** Scheme of the elevator aircraft cable-control system.

From analyzing the stability and maneuverability of airplanes related to the geometrics and kinematics of cable control systems, we conclude: the deflections of the control surfaces are  $\pm 10^\circ$  for  $>90\%$  of the total surface deflection (see Figure 9).

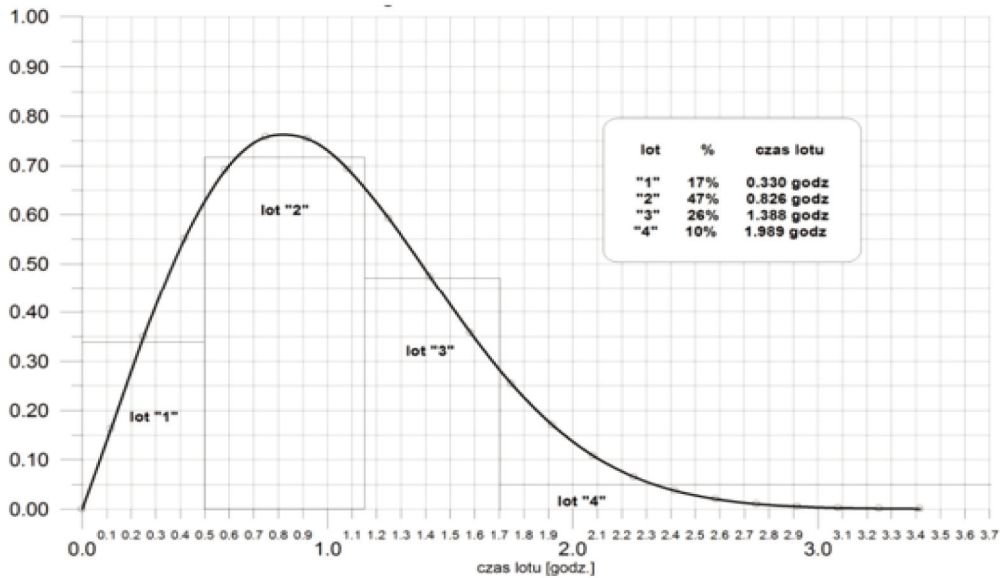


**Figure 7.** Probability density function of flight time distribution for the aircraft commuter category (Kubryn et al., 2018).

The above-mentioned control-cable deformations and displacements indicate that their fatigue lives are much more than those obtained in the tests (Kubryn et al., 2018; Pieróg, 2011).

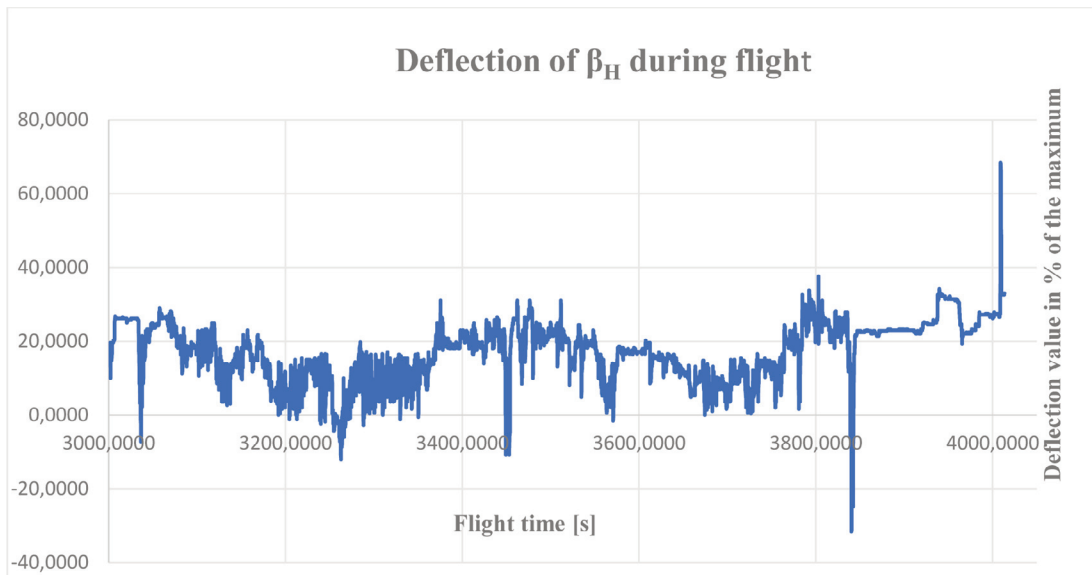


**Figure 8.** Real deflection of the elevator during flight, sampling of 50 Hz. Elaborated based on tests data (Department of Avionics and Control Systems of Rzeszów University of Technology, 2019).

The factor significantly influencing the fatigue life of the cables is a relatively low-value cable load. The method described below and the results of the related tests can be useful for predicting the fatigue life of the cables and defining the diagnostic and adjustment intervals.

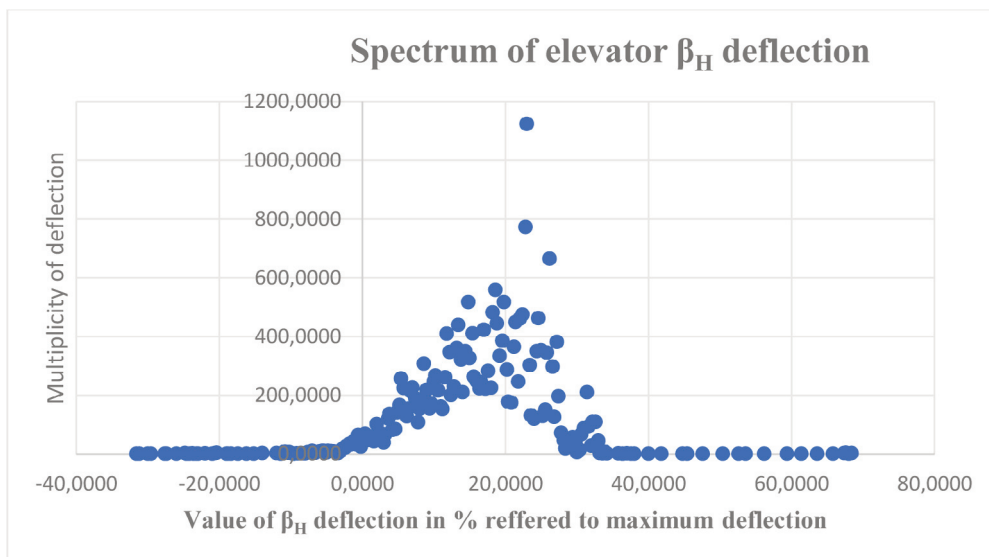


**Figure 9.** Spectrum of rudder deflection. Elaborated on (Department of Avionics and Control Systems of Rzeszów University of Technology, 2019) data. Aerodrome traffic circuit flight. The average value depends on mass and CG location.



## Determining the variability of forces and cable deformation

The force values of the cable-control system can be presented in formulas (5) and (6):

$$P(\alpha_H, \beta_H, v, n, t) = P_W \pm P_M \geq 0 \quad (5)$$

**Note:** Positive tension of the passive cable of control systems means that  $P_W$  should always be greater than  $P_M$  for any permissible flight maneuver (Certification Specifications for CS-23, 2003; Figure 5).

$$P_M = kC_{mz}(\alpha_H, \beta_H, \delta_H, v, \tau) \quad (6)$$

where:

$P(\alpha_H, \beta_H, v, n, t)$  – total forces in the active and passive cables as a function of flight parameters (Figures 6 and 13);

$P_W(t, \tau)$  – pre-tension forces ensuring the positive tension of the passive cable;

$P_M$  – variable forces necessary for control surface deflection;

$\alpha_H$  – angle of attack (Figures 3, 4, and 6);

$\beta_H$  – angle of rudder deflection (Figures 3 and 4);

$\delta_H$  – angle of trim tab deflection (Figure 4);

$v$  – flight speed;

$k$  – calculation of the coefficient of the cable tension forces as a function of the control surface  $C_{mz}$ ,  $\alpha_H$ ,  $\beta_H$ ,  $\delta_H$  deflection (Figures 4, 8 and 9);

$t$  – ambient temperature;

$\tau$  – operational measure, e.g., flight hours;

$C_{mz}$  – hinge moment coefficient  $f(\alpha_H, \beta_H, \delta_H, v, n, t)$  (Eq. (11)), (Figure 10).

Below, the two possible methods of  $C_{mz}$  determination are presented (both based on tunnel research):

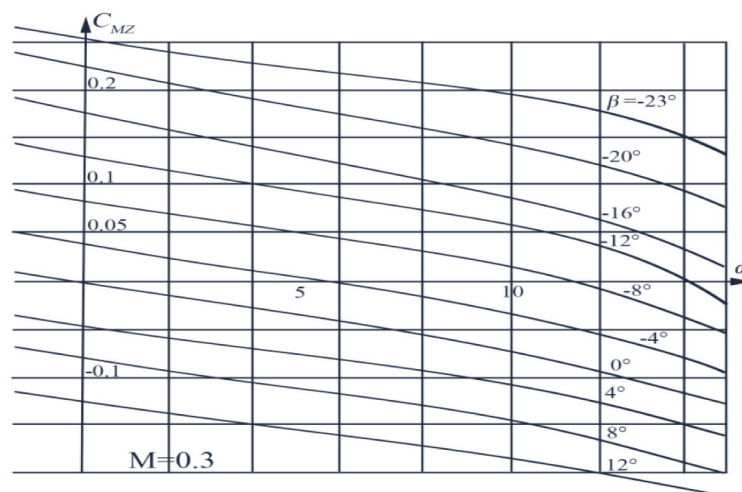


**Figure 10.** An example of the  $C_{mz} = f(\alpha_H, \beta_H, v)$  for specific values of  $K = 0.25$ ,  $R_e = 1.49 \cdot 10^6$ ,  $M_a = 0.3$  (Krzysiak, 1983).

(a) Using the  $C_{mz} = f(\alpha_H, \beta_H, v)$  chart for specific aviation profiles with appropriate values of:  $K$  (Eq. (10); Figure 6),  $R_e, M$ , similarity number (Figure 10);

(b) By the  $C_{mz}$  calculation based on the specified wind tunnel test and using coefficients  $b_1, b_2$ , and  $b_0$  for specific:  $K, R_e, M$  similarity number.

The values of the hinge moments coefficients of the control surfaces determined by the data obtained from tunnel tests are given by formula (7):

$$C_{mz}(R_e, M, K) = b_1 \alpha_H + b_2 \beta_H + b_0 \quad (7)$$

where:

$$b_1 = \frac{\partial C_{mz}}{\partial \alpha} \text{ -- see Figure 11} \quad (8)$$

$$b_2 = \frac{\partial C_{mz}}{\partial \beta} \text{ -- see Figure 12} \quad (9)$$

$b_0$  -- coefficient related to the shape of the tail profile.

$\alpha_H, \beta_H$  -- surface deflection [rad] -- Figure 3.

$$K = \frac{C_{sh}}{L_{ah}} \quad (10)$$

where:

$C_{sh}$  -- rudder chord Figure 4;

$L_{ah}$  -- chord of control surface unit Figure 4;

$R_e, M$  -- Reynolds and Mach similarity numbers.

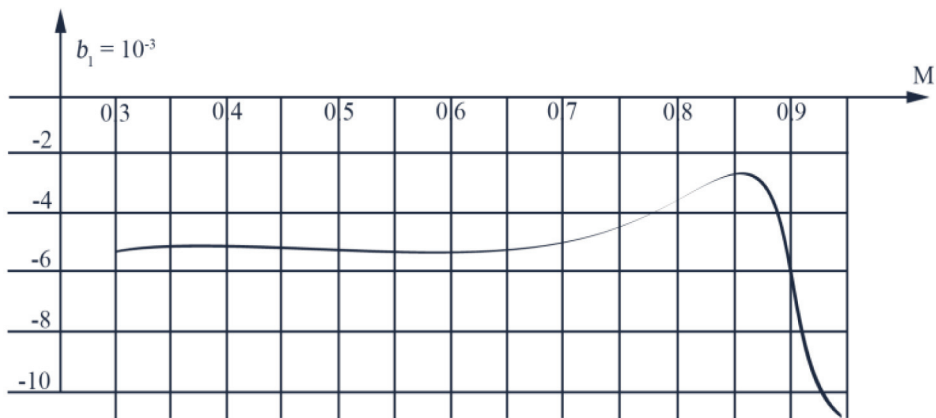


**Figure 11.** An example of  $b_1 = f(M_\infty)$  for the value  $K = 0.25$  (Krzysiak, 1983).

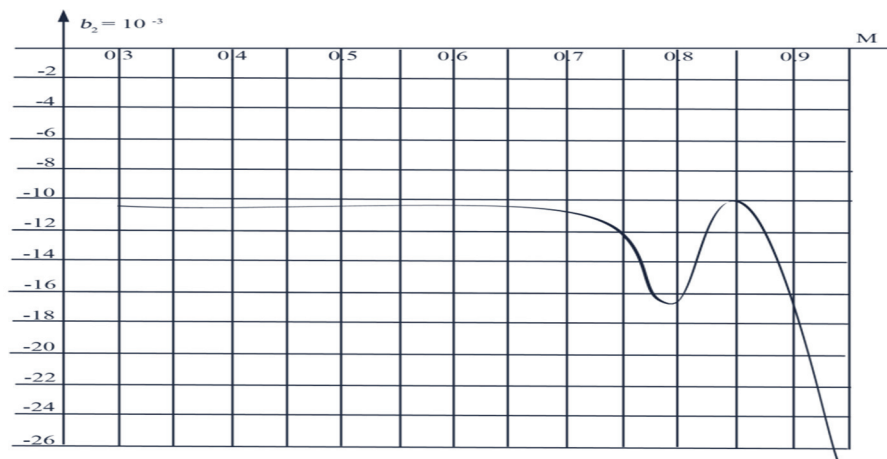


**Figure 12.** An example of  $b_2 = f(M)$  for the value  $K = 0.25$  (Krzysiak, 1983).

Loads of the passive and active cables of the airplane control system should be additionally corrected by the friction forces of the systems (Brzeczek, 2019). The values of the deflections  $\beta_H$  are additionally correlated with the angles of attack  $\alpha_H$  and  $\delta_H$ ; the CG position enables completing the operating spectrum of cable loads (Figure 9).

### Test programs based on the presented idea

The stochastic deflections of the control surfaces,  $\beta_H$ ,  $\delta_H$ , CG, (Figures 7–9.) measured for the typical exploitation profile of the defined airplane's category enable determining the loads spectrum of active and passive cables of the control systems (Figure 5). Test spectra (Figure 9) are related to the flight hours and are not the quantity of cable bending (Department of Avionics and Control Systems of Rzeszów University of Technology, 2019) is presented. The test results are described as a function of flight hours for a given aircraft category (Figures 5 and 9) that should be performed on the critical pulley of the system, i.e., on the greatest bending ( $\max \theta_L$ ) (Figure 13). Test results with additional measurements of the cable elongation and broken wires enable determining the real wear of the cable and pulley (Figure 13) as a function of flight hours. On the basis of the above-mentioned data and the fatigue tests results, formula (11) can be used to determine the fatigue life and diagnostic intervals of the cable system (Tytko, 1998, 2021).

### Strands of the fatigue tests of aviation cable-control systems

The main task involved in conducting the tests of airplane cable-control systems (Figures 6 and 13) is the use of stochastic non-linear loads correlated with cable deformation. The strand allows test cables with different wrap angles, but with the same variable (stochastic) load values, for two or more cables at the same time. The cable loads are applied by angular excitation, and the nonlinearity of the forces changes as a function of the deflection angles and is implemented by spring or hydraulic systems.

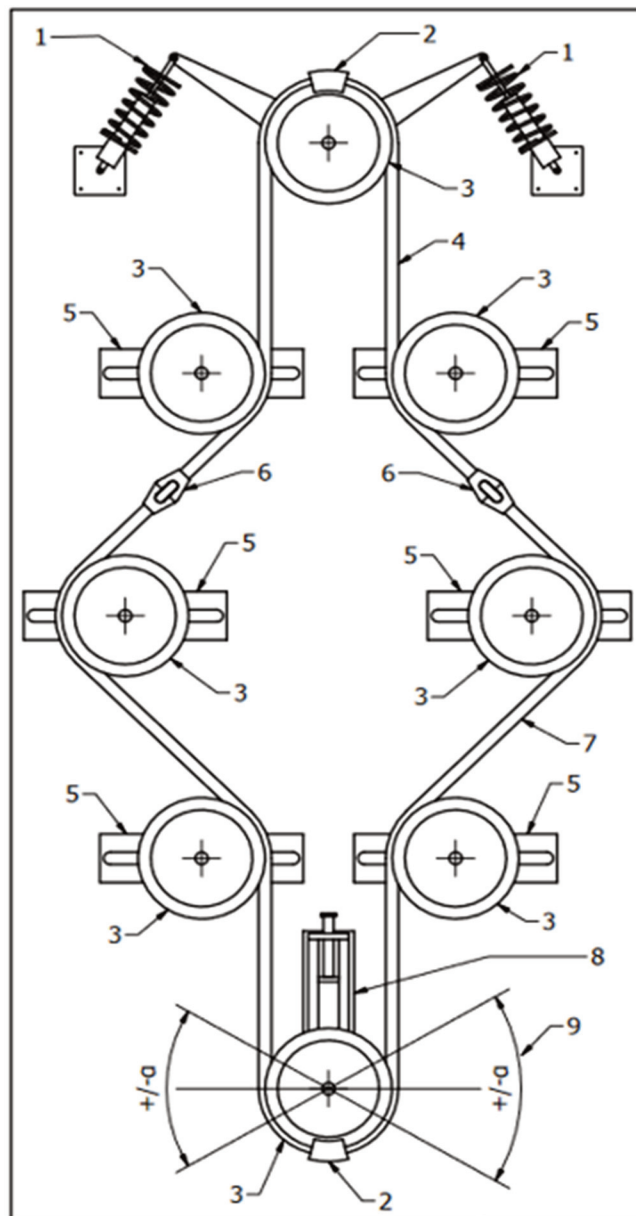


**Figure 13.** Idea of a cable test strand<sup>4</sup>. More than six points of cable testing and inspection. The strand enables the ongoing measurement of cable elongation. The markings in Figure 13 mean: 1 – spring or hydraulic system, simulation of nonlinear hinge change, 2 – cable lock, 3 – pulleys, 4 – cable A, 5 – wrap angle adjustment, 6 – turnbuckle, 7 – cable B, 8 – tensioner (pre-tension value of force), and 9 – stochastic angular displacement ( $\beta_H$  simulation).

<sup>4</sup> Idea of the test strand is the subject of a patent application WIPO ST 10/C PL446415. Idea allows testing more than one cable simultaneously under the same varying loads and various wrap angles on pulleys.

In addition, as emphasized in this paper, the magnitude of the used loads is in correlation with the cable deformation and displacement (Figure 6). Loads and operational spectrum are related to the specific type of airplane control system (Figures 5 and 7) moreover enables to define a critical point on the cable system by the wrap angle displacement (Figure 13). The critical point and fatigue test results should be used to plan the inspection and diagnostic intervals of the aircraft's cable-control systems.

### **Assessment of test results and the fatigue durability of the cable**

A measure of the symptoms of wear of the aviation control-cable systems can be conducted by the cable elongation, reduction of cable diameter, and the broken wires. The measurement test's results will be used for coefficients  $a_1$ ,  $a_2$ , and  $a_3$  for the elongation estimate (Eq. (11)). The course of the curve lengthening of the operated cable similar to the tribological curve and, in accordance with Hankus and Hankus (2006) and Hankus (2004, 2014), can be well described by formula (11):

$$\varepsilon = a_0 + a_1 P (+a_2 P^2 + a_3 P^3) \quad (11)$$

where:

$\varepsilon$  – limit elongation of the cable or rope;

$P$  – tensile load  $P(\alpha, \beta, v, t)$  according to Eq. (5).

The assessment of the elongation of the cable can be determined by the measurement of the pre-tension (Brzęczek, 2019, 2020) as well. Based on the results of measuring the cable elongation, the term for the diagnostics intervals and the cable replacement can be predicted (Brzęczek, 2019).

### **Conclusions**

The presented method for preparing and performing the fatigue tests of an airplane's control-cable system is based on the real loads and deformations of the cable under random values of forces. The loads of the control cables with the associated complex stress of the individual wires, in the presented proposal, are determined by the real values of the hinge moment and other related factors such as the aircraft's operational profile consequence. The proposed solutions are based on flight measurements of  $\alpha_H$ ,  $\delta_H$ , related to the CG position and laboratory wind tunnel profiles test results. The advantage of the proposal is the availability of data related to the real surface deflections of the control systems. A drawback of the proposed solution is the necessity to control the cable tension with the appropriate measurement accuracy, which according to Brzęczek (2019, 2020) is a complex task. The results of the measurement of the line elongation as a function of flight hours give reliable information on the service life of the cable-control system, intervals of inspection, fatigue life forecasting, and decisions concerning cable replacement.

## REFERENCES

- Brzęczek, J. (2019). Examination of Aircraft's cable control systems tension. *Advances in Science and Technology Research*, 13(2), 65–71. <https://doi.org/10.12913/22998624/106238>.
- Brzęczek, J. (2020). Some comments on fatigue life test of aircraft cable control systems. *Fatigue of aircraft Structures*, 2020(12), 102–112. <https://doi.org/10.2478/fas-2020-0010>.
- Certification Specifications for CS-23. (2003). *Normal, performance, aerobatic and local transport aircraft*, November 14, 2003 and related AMC and FTG.
- Department of Avionics and Control Systems of Rzeszów University of Technology. (2019). *Badania w locie samolotu MP-02 Czajka – Rzeszów 2019* – unpublished.
- Hankus, J. (2004) Współczynniki bezpieczeństwa lin wyciągowych nośnych [Factors of safety of hoisting ropes]. *Research Reports. Mining and Environment*, 2/2004, 19–35.
- Hankus, J., & Hankus, Ł. (2006). Nowa metoda badań diagnostycznych lin stalowych z wykorzystaniem magnetycznej pamięci metalu [New method of diagnostic tests of steel ropes using the magnetic memory]. *Research Reports. Mining and Environment*, 2/2006, 107–131.
- Hankus, Ł. (2014) Wzdłużne odkształcenia lin wyciągowych w warunkach złożonych obciążeń cyklicznie zmiennych [Longitudinal strains of hoisting ropes under conditions of complex cyclically changeable loads]. *Przegląd Górniczy*, 2014(5), 101.
- Krzysiak, A. (1983). Eksperymentalne badania momentu zawiasowego w zakresie pod i przydźwiękowych prędkości. *Transactions of the Institute of Aviation*, 1983(94), 3–20.
- Kubryn, M., Gruszecki, H., Pieróg, L., Chodur, J., Pietruszka, J., & Brzęczek, J. (2018). Fatigue life of cables in aircraft flight control systems. *Fatigue of Aircraft Structures*, 2018(10), 53–62. <https://doi.org/10.2478/fas-2018-0005>.
- Pieróg, L. (2011). *Evaluation of PZL M28 05 Airplane Service Life*. Ref. no. DRG/O/W/24/11 PZL Mielec 2011 – unpublished.
- Tytko, A. (1998). *Modelowanie zużycia zmęczeniowego i diagnostyka lin stalowych*. Wydawnictwo AGH Kraków.
- Tytko, A. (2021). *Liny stalowe*. PWN.